A&A 465, 647–650 (2007)
DOI: 10.1051/0004-6361:20066267

Astronomy & Astrophysics

Collisional excitation of doubly deuterated ammonia ND_2H by helium

L. Machin and E. Roueff

Laboratoire Univers et Théories and UMR 8102, Observatoire de Paris-Meudon, 5 place Jules Janssen, 92195 Meudon, France
e-mail: [leandre.machin;evelyne.roueff]@obspm.fr

Received 18 August 2006 / Accepted 26 September 2006

ABSTRACT

Context. Doubly deuterated ammonia has been found in various dense interstellar environments.
Aims. We extend our previous study of singly deuterated ammonia NH_2D collisional excitation by helium to doubly deuterated ammonia ND_2H.
Methods. The presence of two deuterium atoms in the system modifies the symmetry and the expansion coefficients of the intermolecular potential energy surface. We establish the corresponding collision equations.
Results. Cross sections are calculated in the coupled-state (CS) approximation and collisional rate coefficients are given between 5 and 100 K, a range of temperatures that is relevant to interstellar conditions.
Conclusions. These results may be used to interpret the available millimeter and submillimeter observations of ND_2H.

Key words. ISM: general – ISM: molecules – molecular data – molecular processes – scattering

1. Introduction

Doubly deuterated ammonia was detected for the first time by Roueff et al. (2000) towards the dark cloud L 134N via its 1_{10}-1_{01} ortho and para transitions at 110 GHz and subsequently in the protostellar environment L 1689N by Loinard et al. (2001). The submillimeter fundamental transitions were then searched for and found at the Caltech Submillimeter Observatory (CSO) by Roueff et al. (2005), Lis et al. (2006) and on the APEX antenna in Chile by Gerin et al. (2006) towards the Barnard 1 molecular cloud and L 1689N and were shown to be sensitive tracers of the physical conditions of this star-forming region. However, a proper analysis of the observations is required to introduce the appropriate (de)excitation collisional rate coefficients in the statistical equilibrium equations describing the rotational levels of the molecule.

The new accurate intermolecular potential energy surface (PES) for NH_3-He (Hodges & Wheatley 2001) has been used to reevaluate the collisional excitation of NH_3 and NH_2D by He (Machin & Roueff 2005, 2006). In the present paper, we also introduce the modifications caused by the presence of two deuterons in the system and describe the parameters relative to the ND_2H-He system in Sect. 2, both for the evaluation of the PES and the collisional treatment. The cross sections and the corresponding reaction rate coefficients of the ND_2H-He system are given in Sect. 3. We derive the astrophysical implications in Sect. 4.

2. Potential energy surface and collisional treatment

We used the MOLSCAT code version 14 of J. M. Hutson and S. Green to compute the quantal excitation cross sections of ND_2H by He. The present treatment is very similar to what was done for NH_2D-He (Machin & Roueff 2006), so we refer the reader to this paper for the potential surface and the collision equations. We only point out the significant changes compared to NH_2D. Figure 1 displays the two reference frames involved: (i) N, x_N, y_N, z_N used to compute the potential energy surface by Hodges & Wheatley (2001); and (ii) the cartesian frame used in the MOLSCAT code where the origin is centered on the center of mass of the ND_2H molecule:

$$x_N = x' \cos(\gamma) - z' \sin(\gamma) + X_{CM} \quad (1)$$

$$y_N = y' \quad (2)$$

$$z_N = x' \sin(\gamma) + z' \sin(\gamma) + Z_{CM}, \quad (3)$$

where γ is the angle between the z_N and the z' axes and X_{CM} and Z_{CM} are the coordinates of the center of mass of ND_2H in the PES reference frame (x_N, y_N, z_N). The values of γ, X_{CM}, and Z_{CM} are given in Table 1. γ is taken from Cohen & Pickett (1982). X_{CM} and Z_{CM} are calculated for an umbrella angle $\alpha_e = 112.14°$ and for the length of the N-H bond $r_e = 1.9132\ a_0$. These values correspond to the experimental equilibrium geometry given by Benedict et al. (1957) and reported in Hodges & Wheatley (2001). We can see that in the case of ND_2H-He system, the Oy' axis is now perpendicular to the plane of the figure due to the conventions used in the MOLSCAT program.

As for NH_2D-He, we used the "VRTP" procedure in the MOLSCAT program, which provides the expansion coefficients $v_{\lambda\mu}(r')$ of the PES in the body-fixed coordinates:

$$V(r', \theta', \phi') = \sum_{\lambda\mu} v_{\lambda\mu}(r') Y_{\lambda\mu}(\theta', \phi'). \quad (4)$$

The break of the C_{3v} symmetry, relevant to NH_3-He, suppresses the restrictions on the μ values of the $v_{\lambda\mu}(r')$ coefficients. In the present calculations, we included $v_{\lambda\mu}(r')$ until $\lambda = 10$ and all possible values of μ (from 0 to λ) , which allows a satisfactory representation of the PES.

The numerical values of the molecular constants required to represent the ND_2H asymmetric top in MOLSCAT are displayed in Table 2 and taken from CDMS (Müller et al. 2001)

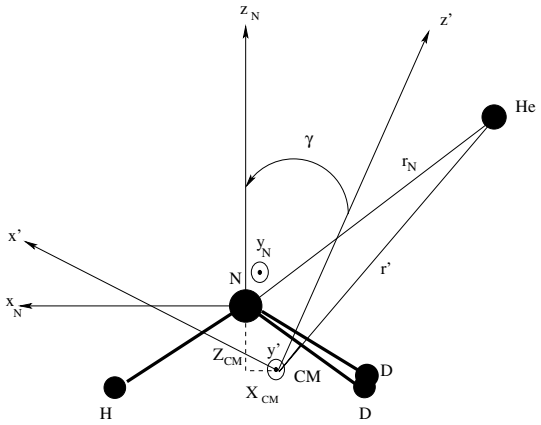

Fig. 1. Relationship between the center of mass reference frame (x', y', z') of ND_2H and the reference frame used by Hodges & Wheatley (2001) for their NH_3-He PES (x_N, y_N, z_N). X_{CM} and Z_{CM} are the coordinates of the center of mass of ND_2H in the PES reference frame. γ is the angle between the z_N and the z' axis. CM indicates the center of mass and N the nitrogen atom.

Table 1. Values of γ, X_{CM}, and Z_{CM} for ND_2H in the PES reference frame (x_N, y_N, z_N).

Parameter	ND_2H
γ (in degrees)	+11.30
X_{CM} (a_0)	−0.0936
Z_{CM} (a_0)	−0.1906

Table 2. Values of the rotational constants $\mathcal{A}$, $\mathcal{B}$, and C and of the centrifugal distortion constants D_{jj}, D_{jk}, and D_{kk} for ND_2H used in this work in units of cm^{-1}.

$\mathcal{A}$	5.3412
$\mathcal{B}$	7.4447
C	3.7533
D_{jj}	3.346×10^{-4}
D_{jk}	-4.931×10^{-4}
D_{kk}	2.164×10^{-4}

and Coudert et al. (1986). The $\mathcal{A}$, $\mathcal{B}$, and C values correspond here respectively to the x', y', and z' axes used in the potential expansion and are different from the A, B, and C defined in spectroscopy, which are in descending order of magnitude. The derived energy-term values of the ten first rotational levels are displayed in Table 3, together with the values computed with a sophisticated Hamiltonian by Coudert & Roueff (2006). The agreement is seen to be satisfactory and equal to about 0.01%.

We do not distinguish ortho and para levels in the Hamiltonian, so ortho and para levels are degenerate in the present treatment and the corresponding collisional excitation probabilities within ortho and para symmetry are identical. We recall that ortho-para transitions are strictly forbidden in such non-reactive collisions. As the reduced mass of ND_2H is higher than the reduced mass of NH_2D, more energy levels than in the NH_3 and NH_2D-He case have to be included for a given total collision energy. The value of the reduced mass μ is taken as 3.3071 amu. We used the coupled states approximation for data production, as for the NH_2D-He system (Machin & Roueff 2006), after checking the validity of the approximation at some specific energies. We display in Table 4 the chosen input parameters used in MOLSCAT. Value of JTOTU = −1 means that MOLSCAT is checking itself for the convergence regarding the maximum J taken into account.

Table 3. Comparison between the energy-term values of the rotational levels of ND_2H calculated by MOLSCAT with the rotational and distortion constants of Table 2 and the mean value of the ortho and para term values from Coudert & Roueff (2006).

Rotational level	Energy (cm^{-1})	
	MOLSCAT	Coudert & Roueff 2006
0_{00}	0.0000	0.0000
1_{01}	9.0939	9.0970
1_{11}	11.1974	11.1904
1_{10}	12.7845	12.7947
2_{02}	26.6595	26.6564
2_{12}	27.7954	27.7788
2_{11}	32.5535	32.5895
2_{21}	38.8640	38.8638
2_{20}	39.4815	39.4967

Table 4. Values of input parameters of MOLSCAT used in our calculations.

Parameter	Value
RMIN	3.0
INTFLG	6
STEPS	20.0
JTOTU	−1
NPTS	14,14

We carefully checked the convergence of the S matrix for the different collision parameters defined in MOLSCAT. The size of the basis set in the PES expansion, i.e. the number of $v_{\lambda\mu}$ included in the calculations, includes terms up to $\lambda = 8$ for energies up to 100 cm^{-1}, which corresponds to 45 $v_{\lambda\mu}$ coefficients. At higher energies, terms up to $\lambda = 10$ have been included so that 66 $v_{\lambda\mu}$ coefficients are effectively used in the basis set. One hundred (121) rotational states have been included in the basis for a collision energy of 100 (400) cm^{-1} corresponding to a maximum energy of 642 (787) cm^{-1}, respectively. A compromise has to be found between the choice of these parameters and the duration of the calculations. Calculations were performed for a total energy range between 10 cm^{-1} and 400 cm^{-1}. The energy step was been varied with increasing collision energy. It is 0.1 cm^{-1} for a total energy range between 10 cm^{-1} and 100 cm^{-1}, 1 cm^{-1} between 100 cm^{-1} and 310 cm^{-1}, 5 cm^{-1} between 310 cm^{-1} and 360 cm^{-1}, and 10 cm^{-1} between 360 cm^{-1} and 400 cm^{-1}.

3. Cross sections and rate coefficients

Figures 2 and 3 display the collisional deexcitation cross sections corresponding to the fundamental transitions $1_{11} \rightarrow 0_{00}$ and $1_{10} \rightarrow 0_{00}$ as a function of the relative kinetic energy between ND_2H and He.

The sharp maxima are due to the opening of new collision channels and they correspond to so-called Feshbach resonances. A small energy step is required in the calculations in order to fully account for these resonances that may affect the results for the rate coefficients at very low temperatures.

The collisional (de)excitation rate coefficients are then obtained as functions of the temperature T via a Maxwellian average of the cross sections times relative velocity:

$$K_{j\tau\rightarrow j'\tau'}(T) = \left(\frac{8k_BT}{\pi\mu}\right)^{\frac{1}{2}}\left(\frac{1}{k_BT}\right)^2 \times \int_o^\infty \sigma_{j\tau\rightarrow j'\tau'}(E_{tot})\, E\, \exp\left(-\frac{E}{k_BT}\right) dE, \quad (5)$$

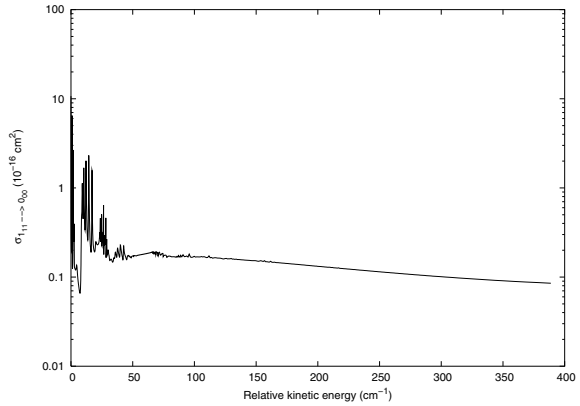

Fig. 2. Collisional deexcitation cross section σ (in 10^{-16} cm^2) as a function of the relative kinetic energy for the transition $1_{11} \rightarrow 0_{00}$ of ND_2H.

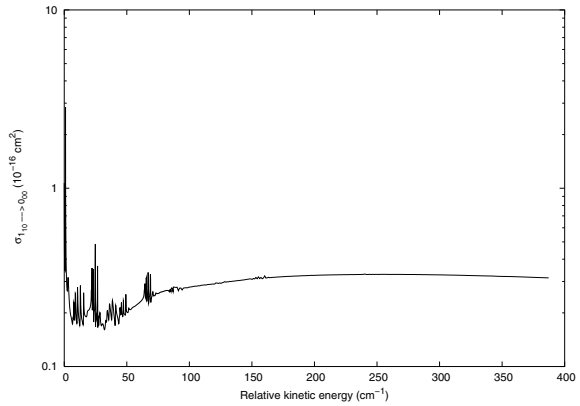

Fig. 3. Collisional deexcitation cross section σ (in 10^{-16} cm^2) as a function of the relative kinetic energy for the transition $1_{10} \rightarrow 0_{00}$ of ND_2H.

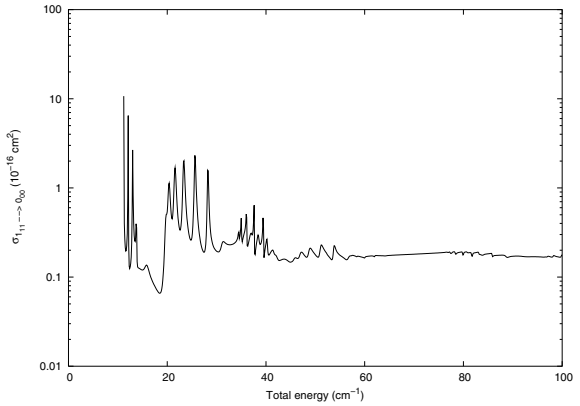

Fig. 4. Resonance structure in the cross section σ of the $1_{11} \rightarrow 0_{00}$ transition.

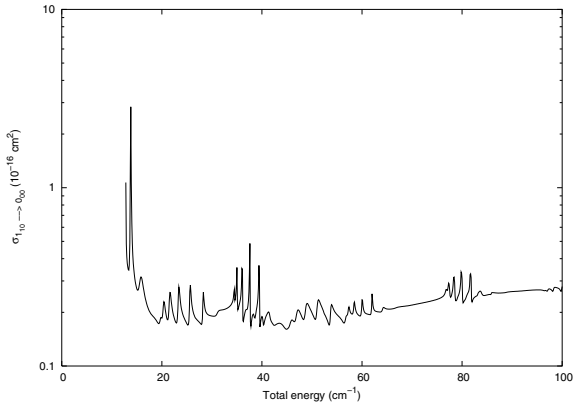

Fig. 5. Resonance structure in the cross section σ of the $1_{10} \rightarrow 0_{00}$ transition.

where E is the relative kinetic energy, k_B the Boltzmann constant, and μ the reduced mass of the ND_2H-He system. As the integration should be performed until reaching an infinite value of the relative kinetic energy, actual calculations introduce a maximum value that should be significantly higher than the thermal energy given approximately by $k_B T$, so that the decreasing exponential appends a negligible contribution. As cross sections were been computed until 400 cm^{-1}, we calculated the rate coefficients for temperatures between 5 K and 100 K, which are relevant for the cold prestellar cores where these transitions are observed. We checked the detailed balance via independent integrations of the excitation and de-excitation cross-sections in order to validate our results. The detailed balance conditions on the rate coefficients are then verified with an error not exceeding 0.6%.

We display in Table 5 the values of the Einstein coefficients and the rate coefficients corresponding to transitions of ND_2H induced by He collisions, involving the lowest energy levels for temperatures between 5 and 100K. We note that the Einstein coefficients of ortho and para transitions may be different by a factor up to a few. The main origin of this discrepancy lies in the ν^3 factor in the Einstein coefficient formula. As an exemple, the frequencies of the para and ortho $2_{12} \rightarrow 2_{02}$ transitions are 28.562 and 38.739 GHz respectively, leading to a factor of 2.5 in the Einstein coefficients from the ν^3 ratio, as one can see in Table 5. The temperature variation is smooth, as one can see from the values displayed in Table 5, and collisional de-excitation rate coefficients increase slightly with temperature.

4. Astrophysical implications

Molecular hydrogen is the main constituent of interstellar molecular clouds, and the interpretation of astrophysical spectra requires knowledge of the collision rates of molecules with molecular hydrogen. Helium is often considered a prototype for molecular hydrogen in its para form, $j = 0$, which is probably the most abundant populated level in cold dark interstellar clouds. Then, rate coefficients for ND_2H-para-H_2 can be tentatively estimated from those involving He as the product of the rate coefficients for ND_2H-He by the square root of the ratio of the reduced masses (here 1.3469).

Astrophysicists introduced the concept of a critical density for a specific transition as the ratio between the Einstein coefficients A_{if} and the rate coefficients K_{if} for a specific collider. This value sets the limit of the perturber density above which the transitions may be thermalized. Table 6 displays the estimated values of the critical densities of H_2 thus derived for some specific transitions. We see that the critical densities corresponding to the two fundamental transitions ($1_{11} \rightarrow 0_{00}$ and $1_{10} \rightarrow 0_{00}$) are different by a factor of about 60 at 10K, which is about a factor of 2 times the ratio of the Einstein coefficients. Such differences may have profound consequences on the interpretation of these two transitions, which are both observable from the ground (Lis et al. 2006; Gerin et al. 2006) at 335 and 389 GHz, respectively, as the corresponding upper levels may not be accounted for by the same excitation temperature. We also note that the critical density derived for the 110 GHz transitions is about 6×10^5 cm^{-3}, a value close to the derived density of L134N where this transition was been detected for the first time.

Table 5. Einstein coefficients and rate coefficients for ND_2H-He for different temperatures, with only de-excitation transitions considered. Numbers in parentheses correspond to the power of ten. Einstein coefficients are taken from the CDMS database (Müller et al. 2001) and are given for the *ortho* and *para* transitions.

Transition	Einstein coefficients A_{if} (s^{-1})		Rate coefficients K_{if} ($cm^3\ s^{-1}$)					
	ortho	*para*	5 K	10 K	25 K	50 K	75 K	100 K
$1_{11} \rightarrow 0_{00}$	1.29(–5)	1.47(–5)	6.67(–13)	9.88(–13)	1.14(–12)	1.21(–12)	1.27(–12)	1.32(–12)
$1_{11} \rightarrow 1_{01}$	2.36(–6)	3.82(–6)	9.49(–13)	1.30(–12)	1.49(–12)	1.98(–12)	2.55(–12)	3.03(–12)
$1_{10} \rightarrow 0_{00}$	4.82(–4)	4.43(–4)	4.67(–13)	5.60(–13)	8.59(–13)	1.36(–12)	1.82(–12)	2.17(–12)
$1_{10} \rightarrow 1_{01}$	6.96(–7)	7.96(–7)	5.94(–13)	8.51(–13)	1.20(–12)	1.48(–12)	1.65(–12)	1.76(–12)
$1_{10} \rightarrow 1_{11}$	–	–	7.99(–12)	7.07(–12)	6.09(–12)	5.78(–12)	5.75(–12)	5.75(–12)
$2_{02} \rightarrow 0_{00}$	–	–	1.96(–12)	2.19(–12)	2.28(–12)	2.55(–12)	2.83(–12)	3.05(–12)
$2_{02} \rightarrow 1_{01}$	–	–	6.76(–13)	6.90(–13)	5.25(–13)	4.35(–13)	4.11(–13)	4.00(–13)
$2_{02} \rightarrow 1_{11}$	1.94(–5)	2.07(–5)	1.37(–11)	1.23(–11)	1.24(–11)	1.46(–11)	1.66(–11)	1.79(–11)
$2_{02} \rightarrow 1_{10}$	5.97(–5)	6.34(–5)	3.97(–13)	4.38(–13)	4.14(–13)	4.19(–13)	4.72(–13)	5.32(–13)
$2_{12} \rightarrow 1_{01}$	–	–	1.69(–11)	1.61(–11)	1.64(–11)	1.88(–11)	2.10(–11)	2.24(–11)
$2_{12} \rightarrow 1_{11}$	–	–	2.08(–12)	1.81(–12)	1.62(–12)	1.61(–12)	1.64(–12)	1.66(–12)
$2_{12} \rightarrow 1_{10}$	–	–	2.72(–13)	3.42(–13)	4.52(–13)	5.79(–13)	7.60(–13)	9.37(–13)
$2_{12} \rightarrow 2_{02}$	8.69(–7)	3.49(–7)	1.93(–12)	1.63(–12)	1.74(–12)	2.42(–12)	3.15(–12)	3.75(–12)
$2_{11} \rightarrow 1_{01}$	2.52(–3)	2.63(–3)	1.17(–12)	1.07(–12)	1.21(–12)	1.68(–12)	2.14(–12)	2.51(–12)
$2_{11} \rightarrow 1_{11}$	–	–	3.79(–11)	3.89(–11)	3.94(–11)	4.04(–11)	4.10(–11)	4.09(–11)
$2_{11} \rightarrow 1_{10}$	6.49(–5)	7.07(–5)	1.67(–12)	1.64(–12)	1.59(–12)	1.65(–12)	1.72(–12)	1.76(–12)
$2_{11} \rightarrow 2_{02}$	2.27(–6)	2.13(–6)	5.41(–12)	6.14(–12)	8.83(–12)	1.22(–11)	1.46(–11)	1.61(–11)
$2_{11} \rightarrow 2_{12}$	–	–	6.30(–12)	5.77(–12)	5.11(–12)	5.00(–12)	5.19(–12)	5.41(–12)
$2_{21} \rightarrow 0_{00}$	–	–	1.67(–12)	1.65(–12)	1.75(–12)	2.04(–12)	2.30(–12)	2.48(–12)
$2_{21} \rightarrow 1_{01}$	–	–	2.85(–11)	2.90(–11)	2.92(–11)	3.02(–11)	3.08(–11)	3.09(–11)
$2_{21} \rightarrow 1_{11}$	4.20(–3)	4.18(–3)	1.97(–12)	2.00(–12)	2.24(–12)	2.74(–12)	3.19(–12)	3.51(–12)
$2_{21} \rightarrow 1_{10}$	2.47(–4)	1.05(–4)	1.20(–12)	1.24(–12)	1.43(–12)	1.83(–12)	2.20(–12)	2.48(–12)
$2_{21} \rightarrow 2_{02}$	–	–	7.39(–12)	6.78(–12)	6.05(–12)	6.02(–12)	6.34(–12)	6.64(–12)
$2_{21} \rightarrow 2_{12}$	8.15(–6)	5.86(–6)	4.49(–12)	5.25(–12)	6.67(–12)	8.46(–12)	1.00(–11)	1.11(–11)
$2_{21} \rightarrow 2_{11}$	2.87(–5)	2.55(–5)	8.29(–13)	9.17(–13)	1.23(–12)	1.68(–12)	2.07(–12)	2.37(–12)
$2_{20} \rightarrow 0_{00}$	–	–	1.21(–11)	1.18(–11)	1.21(–11)	1.34(–11)	1.44(–11)	1.50(–11)
$2_{20} \rightarrow 1_{01}$	–	–	4.56(–12)	4.58(–12)	4.69(–12)	5.09(–12)	5.46(–12)	5.70(–12)
$2_{20} \rightarrow 1_{11}$	2.36(–4)	9.21(–5)	6.42(–13)	7.07(–13)	9.59(–13)	1.36(–12)	1.68(–12)	1.92(–12)
$2_{20} \rightarrow 1_{10}$	4.42(–3)	4.47(–3)	2.23(–12)	2.20(–12)	2.40(–12)	3.01(–12)	3.58(–12)	4.00(–12)
$2_{20} \rightarrow 2_{02}$	–	–	1.51(–11)	1.45(–11)	1.31(–11)	1.23(–11)	1.21(–11)	1.18(–11)
$2_{20} \rightarrow 2_{12}$	5.76(–5)	6.57(–5)	9.00(–13)	9.93(–13)	9.98(–13)	1.12(–12)	1.27(–12)	1.39(–12)
$2_{20} \rightarrow 2_{11}$	3.93(–6)	2.46(–6)	1.24(–12)	1.42(–12)	1.98(–12)	2.87(–12)	3.64(–12)	4.22(–12)
$2_{20} \rightarrow 2_{21}$	–	–	1.44(–12)	1.33(–12)	1.35(–12)	1.73(–12)	2.16(–12)	2.50(–12)

Table 6. Estimated critical density for some *ortho* and *para* transitions of ND_2H with H_2 at 10 K.

Transition	Critical density (cm^{-3})	
	ortho	*para*
$1_{11} \rightarrow 0_{00}$	9.69×10^6	1.11×10^7
$1_{11} \rightarrow 1_{01}$	1.35×10^6	2.18×10^6
$1_{10} \rightarrow 0_{00}$	6.39×10^8	5.87×10^8
$1_{10} \rightarrow 1_{01}$	6.07×10^5	6.95×10^5
$2_{02} \rightarrow 1_{11}$	1.17×10^6	1.25×10^6
$2_{02} \rightarrow 1_{10}$	1.01×10^8	1.08×10^8
$2_{12} \rightarrow 2_{02}$	3.96×10^5	1.59×10^5
$2_{11} \rightarrow 1_{01}$	1.75×10^9	1.82×10^9
$2_{11} \rightarrow 1_{10}$	2.94×10^7	3.20×10^7
$2_{11} \rightarrow 2_{02}$	2.75×10^5	2.58×10^5
$2_{21} \rightarrow 1_{11}$	1.56×10^9	1.55×10^9
$2_{21} \rightarrow 1_{10}$	1.48×10^8	6.29×10^7
$2_{21} \rightarrow 2_{12}$	1.15×10^6	8.29×10^5
$2_{21} \rightarrow 2_{11}$	2.32×10^7	2.06×10^7
$2_{20} \rightarrow 1_{11}$	2.48×10^8	9.67×10^7
$2_{20} \rightarrow 1_{10}$	1.49×10^9	1.51×10^2
$2_{20} \rightarrow 2_{12}$	4.31×10^7	4.911×10^7
$2_{20} \rightarrow 2_{11}$	2.06×10^6	1.29×10^6

The values of the rate coefficients are available on request and will be part of the Basecol database[1] operated at the Observatoire de Paris by M.L. Dubernet.

[1] Basecol, `http://amdpo.obspm.fr/basecol/`

Acknowledgements. We are grateful to Marie-Lise Dubernet from LERMA, Observatoire de Paris, and Pierre Valiron from the Laboratoire d'Astrophysique de Grenoble for useful discussions. This work is part of the tasks defined in the European FP6 network "The Molecular Universe". Support from the National Program "PCMI" is gratefully acknowledged.

References

Benedict, W. S., Gailar, N., & Plyler, E. K. 1957, Can. J. Phys., 35, 1235
Cohen, A. E., & Pickett, H. M. 1982, J. Mol. Spectrosc., 93, 83
Coudert, L., Valentin, A., & Henry, L. 1986, J. Mol. Spectrosc., 120, 185
Coudert, L., & Roueff, E. 2006, A&A, 449, 855
Gerin, M., Lis, D. C., Philipp, S., et al. 2006, A&A, 454, L63
Hodges, M. P., & Wheatley, R. J. 2001, J. Chem. Phys., 114, 8836
Lis, D. C., Gerin, M., Roueff, E., Vastel, C., & Phillips, T. G. 2006, ApJ, 636, 916
Loinard, L., Castets, A., Ceccarelli, C., Caux, E., & Tielens, A. G. G. M. 2001, ApJ, 552, L163
Machin, L., & Roueff, E. 2005, J. Phys. B: At. Mol. Opt. Phys., 38, 1519
Machin, L., & Roueff, E. 2006, A&A, 460, 953
Hutson, J. M., & Green, S. 1995, MOLSCAT computer code, version 14, distibuted by collaborative computational project No.6 of the Science and Engineering Research Council, UK
Müller, H. S. P., Thorwirth, S., Roth, D. A., & Winnewisser, G. 2001, A&A, 370, L49
Roueff, E., Tiné, S., Coudert, L. H., et al. 2000, A&A, 354, 63
Roueff, E., Lis, D. C., van der Tak, F. F. S, Gerin, M., & Golsmith, P. F. 2005, A&A, 438, 585